

Objective Evaluation of Skin Texture Condition by Image Analysis

Toshiyuki Tanaka¹ and Haruna Suzuta¹

Keio University, Yokohama, 223-8522, Japan,
tanaka@appi.keio.ac.jp,

WWW home page: <http://isp.appi.keio.ac.jp>

Abstract. This paper presents an analysis method that extracts the features of “skin texture” and “unevenness of skin color” from skin images. We determine the effective features for the evaluation of skin texture using a two-sample t-test on the cheek and underside of the chin. The results show that the total number of cristae cutis as well as the mean and standard deviation of their area are effective features for skin texture analysis. In addition, the maximum value of an a^* image as well as the standard deviation and kurtosis value of a b^* image are effective features for assessing the unevenness of skin color. The results of tests show that the standard deviation of the area with changing colors is an effective feature for skin texture analysis.

Keywords: skin analysis, skin texture, color unevenness, blotch, skin pore, cheek, underside of the chin

1 Introduction

Conventional skin texture evaluation is mostly performed by skilled beauty technicians, and is performed using visual assessment. In recent years, skin texture can be measured objectively using the optical characteristics of the skin and newly developed measurement approaches [1-5]. However, even now, most systems require great care and are not suitable for general use. Moreover, it is difficult to extract skin texture, area, and color unevenness and assess the skin quantitatively.

In this paper, we focus on “skin texture” and “color unevenness” of skin images, which characterize the skin condition well. Further, we aim to determine the quantitative features that are available for measuring skin texture. An intensity image was investigated for skin texture analysis and a polarized light image was investigated for color unevenness in [6]. Fine body hair and skin pores affect color unevenness [7, 8]. We use frequency information [9] to extract skin pores. New approaches are proposed for the extraction of color information and color assessment, and effective features are selected using discriminant analysis. Moreover, objective assessment is performed by comparing the skin of the cheek with that of the chin.

2 Skin Texture Experiments

2.1 Photographing Skin

In this study, a microscope (USB Microscope M3, Scalar Corporation) [10] is used for taking skin images (Fig. 1). The resolution of the images is 1,280 x 1,024 pixels. As shown in Fig. 2, the LED of this microscope has a polarized light filter and controls the light reflected from the object. Texture images of the skin surface, which can be concave or convex, are clearly obtained when the polarized filter is used. Blemish information is better obtained when the polarized filter is not used. Both images are required to evaluate the texture of skin.

2.2 Imaging Regions

The condition of the skin degrades as each person ages. However, these conditions are different at different sites. We define the skin on the cheek to be the average skin condition on the face and the skin under the chin to be the most youthful part. The cheek and chin parts are photographed for each subject using both the polarized and non-polarized modes of the microscope. Figure 3 shows an example of cheek and chin images of the same person. The chin image has better condition than the cheek image with respect to skin texture. The image format is 32-bit PNG, and the resolution of the image is 458 x 334 pixels.

2.3 Subjects of the Experiments

In this study, all the subjects were graduate school students: 16 males and 20 females. We first preprocessed the image. Because we determined that male facial hair affects the subsequent results, we omitted the images of male faces, and analyzed the skin texture of females only.

2.4 Experiment Conditions

Skin condition is greatly affected by the weather. In the present study, we collected skin images in the autumn. The date collection covered a period of two days, except for the part of the photo.



Fig. 1. USB Microscope M3

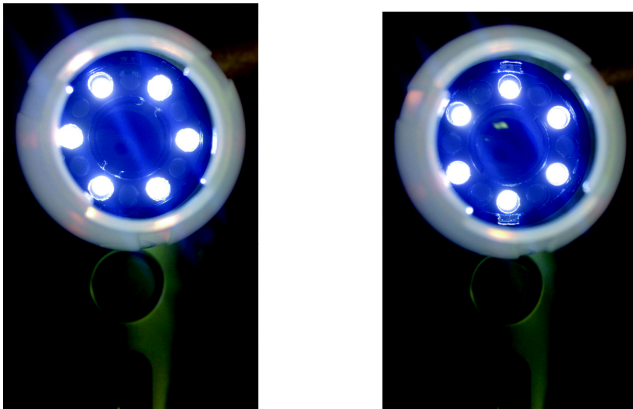


Fig. 2. Mechanism of lighting.

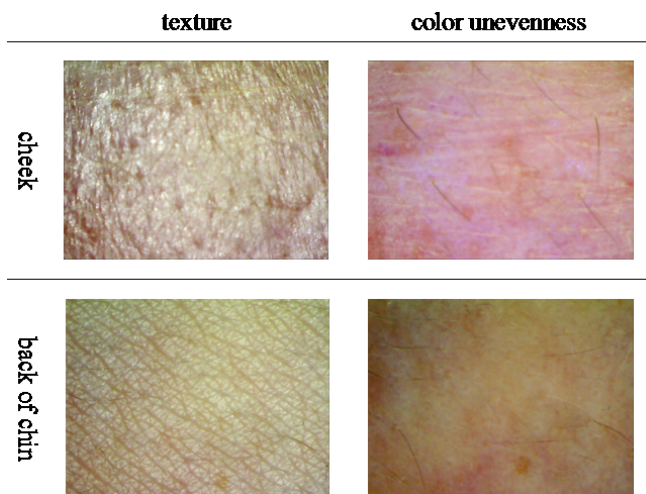


Fig. 3. Example of cheek and chin images

Day 1: 2014 November 13 (10:00-19:00)

Day 2: 2014 November 14 (10:00-19:00)

The average air temperature and precipitation on these days were as follows.

Day 1: Average air temperature 16.97 °C, precipitation 0.0 mm

Day 2: Average air temperature 14.35 °C, precipitation 0.0 mm

3 Proposed Method for Skin Texture Measurement

Figure 4 shows the flowchart of the proposed method. First, texture and color unevenness images are collected by the microscope. The images are preprocessed by filtering and the skin features are quantitatively computed from the obtained images. Discriminant analysis is performed using the computed skin features. Finally, the number, fineness, and proportionality of the skin grit are obtained from the final skin grit images. The color unevenness and spots on the skin are computed from the skin grit images.

3.1 Skin grit

The following four preprocessing steps performed to obtain skin grit images.

(1) Conversion of the image from RGB color space to $L^*a^*b^*$ color space

(2) Adaptive binarization for the L^* component image

(3) Component labeling

(4) Removal of the outliers of the feature values

Each of these preprocessing steps are described below.

(1) Conversion of the image from RGB color space to $L^*a^*b^*$ color space

It is difficult to extract the skin grit from an image in RGB color space, because the difference in hue between grooves in the skin and pichu on the skin is small. In this study, we focus on the difference of the intensity between the grooves and pichu on the skin using CIE1976 $L^*a^*b^*$ color space.

(2) Adaptive binarization

Because the light on the head of the camera illuminates the area that is imaged, the obtained images have color unevenness. It is difficult to extract the features using a fixed threshold on such images. Therefore, adaptive binarization is used, in which the threshold changes according to each pixel of the input image.

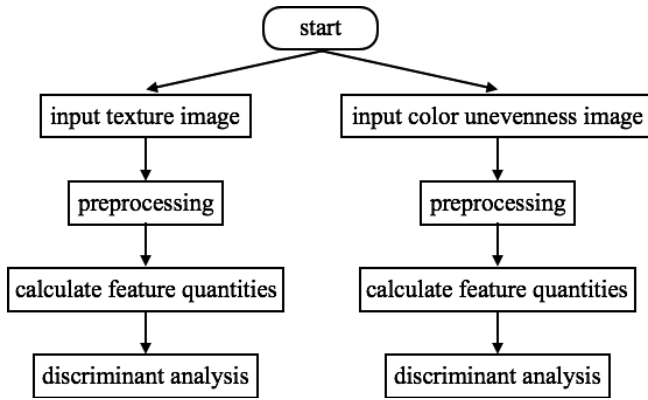


Fig. 4. Flowchart of the proposed method

We denote a Gaussian filter of size of N as M . The adaptive binarization I_{adaptive} of an arbitrary pixel (x, y) is computed by

$$I_{\text{adaptive}}(x, y) = M \otimes I(x, y) - 2. \quad (1)$$

In the (1), \otimes is the filter operation on arbitrary pixel $I(x, y)$. A value of 1 is assigned to the pixel if the intensity is more than the threshold, and a value of 0 is assigned to the pixel otherwise. The subtracted constant reduces the effects of noise and flicker in the background region, specially when the intensity of the near-field region resembles that of the object. In this study, $N = 15 \times 15$ pixels and the subtraction constant is set to be 2 empirically.

(3) Component labeling

Because there are many connected components in one image, the components must be numbered for the subsequent processing. Here, the component labeling is performed to number each connected component.

(4) Removal of the outliers of the feature values

The regions with an area of more than 500 pixels and less than 5 pixels are removed from the set of labeled regions. Regions with an area of more than 500 pixel correspond to unsuitably illuminated regions near the edge of the image, and regions with an area of less than 5 pixels correspond to regions that are much smaller than skin grit. The threshold levels are decided empirically using comparison with the original image. Figure 5 shows examples of the obtained skin grit.

In Figure 5, the red lines indicate the connected components after the removal of outlier connected components. The total number of objects (skin grit) as well as the average and standard deviation of the component areas

are computed from the preprocessed images. These values correspond to the proportionality index of the skin grit.

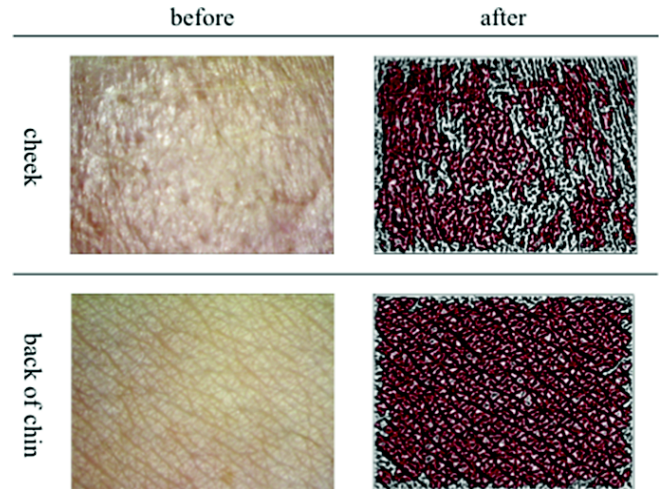


Fig. 5. Example of skin grit extraction

3.2 Color unevenness of the skin

The conversion of RGB images into $L^*a^*b^*$ and the removal of noise (fine facial hair) are performed before the evaluation of the color unevenness. In the following, the noise removal is described.

Especially in chin images, fine facial hair sometimes influences the subsequent results. Therefore, we formulate the process of fine hair removal from the image as noise removal. First, a mask image is constructed for the fine hair, and is superimposed on the original image. The obtained image is interpolated with respect to the fine hair parts, as shown in Fig. 6. In this figure, the red pixel is the reference pixel. The average value is assigned to the reference pixel by raster scanning the whole image and by checking the skin density of the nearest neighbors.

The maximum value, standard deviation, kurtosis, and skewness of the pixel density are computed as the color unevenness features.

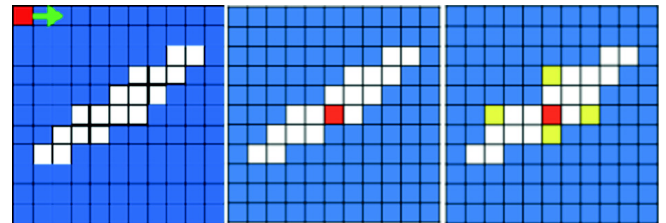


Fig. 6. Interpolation of pixel density for noise removal

3.3 Blotches and skin pores

The conversion of RGB images into $L^*a^*b^*$ space, noise removal, construction of a frequency image, measurement of the frequency distribution are the preprocessing steps needed for blotch and skin pore evaluation. In the following, the construction of the frequency image and measurement of the frequency distribution are detailed.

(1) Frequency image

A frequency image is an image in which the frequency of occurrence of the pixel value in the original image is shown, which is the color frequency information. Although a histogram is often used to represent frequency information in an image, the histogram has the disadvantage that the position information is lost in the process of computation. The frequency image has both the position and frequency information. The original and frequency images are shown in Fig. 7.

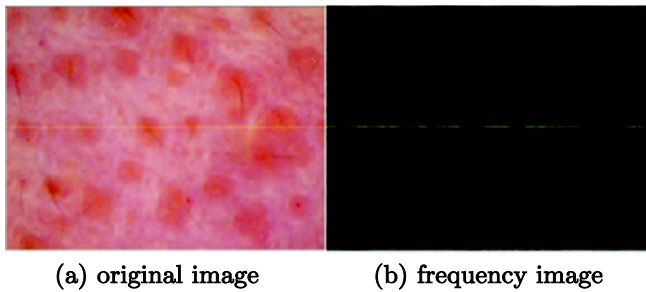


Fig. 7. Original image in RGB color space and the resulting frequency image

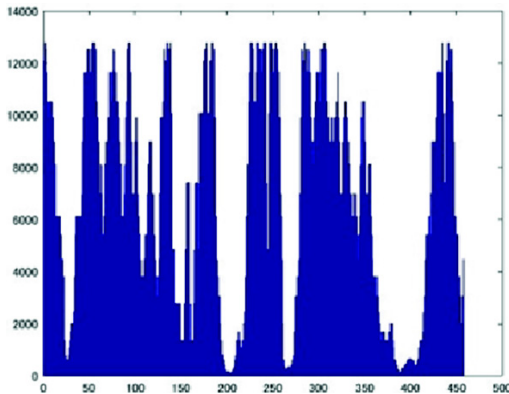


Fig. 8. Profile of the frequency image

(2) Frequency distribution measurement

In order to estimate the frequency image, we make a profile of the frequency image in the middle row of the image, as shown in Fig. 8.

The peaks and valleys of the graph correspond to the parts in which the color unevenness is high. When the valleys are deep and broad, the color unevenness is large and dark.

We use four thresholds at the frequency values of 5,000, 10,000, 15,000, and 20,000 in Fig. 8. The number of peaks and valleys, width of the valleys, and the standard deviation of the valley width are computed at each threshold. When the frequency value is small and the above feature values are distinct, the color unevenness of an aggregated uneven region appears dominantly. The threshold value is empirically decided from the shape of profile image and the condition of the blotches and skin pores. In the subsequent analysis, we define the threshold value of 5,000 to be Level 1, 10,000 to be Level 2, 15,000 to be Level 3, and 20,000 to be Level 4. Although only one profile image in the middle of the image is demonstrated above, the same processing is performed over the entire region and the average values are computed for each index. The averaged indexes correspond to the number, area, and standard deviation of the area.

3.4 Discriminant analysis

A t-test at a 5% significance level was performed for the features obtained by skin grit, color unevenness, and skin pore processes. We then determined the effective features that have a significant difference between the index values in the cheek image and the chin image.

4 Results

The results of the test for the skin grit features are shown in Table 1, those of the color unevenness features are shown in Table 2, and those of the blotch and skin pore features are shown in Table 3. The values in the tables show the p values of the tests. In Table 1, the total number of the skin grit components, the average area of the grit components, and the standard deviation of their area are effective features for the assessment of skin grit. Table 2 shows that the maximum frequency value and standard deviation in the a^* component images are effective for analysis, and that the standard deviation and kurtosis of the b^* component images are also effective. Furthermore, Table 3 shows that the standard deviation of Level 1 in the a^* component image as well as the average value and standard deviation of Levels 1, 3, and 4 are effective features.

Table 1. Results of skin texture feature discriminant analysis

	Total number	Mean area	Area std.
p value	1.3e-07	2.5e-04	3.9e-10

Table 2. Results of color unevenness feature discriminant analysis

(a) L* component image

	Max	Std.	Kur.	Skw.
p value	0.80	0.90	0.68	0.60

(b) a* component image

	Max	Std.	Kur.	Skw.
p value	7.05e-04	1.43e-02	5.70e-01	7.05e-01

(c) b* component image

	Max	Std.	Kur.	Skw.
p value	1.94e-01	8.90e-03	8.18e-07	3.07e-01

Table 3. Results of blotch and skin pore feature discriminant analysis

(a) L* component image

	Number	Area mean	Std. area
Level 1	0.78	0.63	0.64
Level 2	0.85	0.81	0.80
Level 3	0.68	0.54	0.57
Level 4	0.43	0.09	0.16

(b) a* component image

	Number	Area mean	Std. area
Level 1	0.32	0.06	0.02
Level 2	0.67	0.53	0.64
Level 3	0.16	0.12	0.14
Level 4	0.46	0.11	0.25

(c) b* component image

	Number	Area mean	Std. area
Level 1	0.04	0.03	0.05
Level 2	0.20	0.42	0.26
Level 3	0.09	0.03	0.02
Level 4	0.08	0.01	0.01

5 Conclusion

In this study, we proposed an analysis method to extract skin texture and skin color unevenness features from magnified images of skin. In addition, we obtained effective features for the evaluation of skin condition by conducting two-sample t-tests on features extracted from images of the cheek and underside of the chin. As a result, for skin texture, we found that the total number of cristae cutis as well as the mean and standard deviation of those areas are effective features. For skin color unevenness, the maximum value of the a* image as well as the standard deviation and kurtosis of the b* image are effective. In addition, we created frequency images of colors for L*, a*, and b* images and analyzed the distribution and depth of the color. In this way, we obtained features for color unevenness, especially changes in colors, which correspond to blotches and skin pores. The test results show that the standard deviation of the area with color changes whose color frequencies are under 20,000 in an a* image and the mean and standard deviation of the area with color changes whose color frequencies are under 20,000, 10,000, and 5,000 in a b* image are effective.

References

1. Y. Baba, T. Mashita, Y. Mukaigawa, and Y. Yagi. Statistical Analysis of Human Skin Based on Reflection and Scattering Characteristics. IPSJ SIG Technical Report. 2009, vol. CVIM-167, no. 22 (2009)
2. H. Kobayashi, T. Hashimoto, K. Yamazaki, Y. Hirai. Proposal of Quantitative Index of Skin Texture by the Image Processing and Its Practical Application, Transactions of Japan Society of Mechanical Engineers Series C, vol. 76, no. 764, pp. 138-145 (2010) (in Japanese)
3. M. Nishioka. Measurement of Skin Texture Using Genetic Picture Analysis. The Institute of Electronics, Information and Communication Engineers. 2010-6, vol. 104, no. 140, pp. 65-69 (2010)
4. A. Sparavigna, R. Marazzato, An image processing analysis of skin textures, Skin Research and Technology, vol. 16, no. 2, pp. 161-167 (2010)
5. N. Ojima, I. Fujiwara, Y. Inoue, N. Tsumura, T. Nakaguchi, K. Iwata. Analysis on Unevenness of Skin Color Using the Melanin and Hemoglobin Components Separated by Independent Component Analysis of Skin Color Image, Proceedings of the SPIE, vol. 7897, 10.1117/12.873494

6. R. Rox Andescon. Polarized Light Examination and Photography of the Skin. *Arch. Dermatol.* 1991, vol. 7, no. 127, pp. 1000-1005 (1991)
7. N. Arakawa, H. Ohnishi, Y. Masuda. Development of Quantitative Analysis for the Micro-Relief of the Skin Surface Using a Video Microscope and Its Application to Examination of Skin Surface Texture, *J. Soc. Cosmet. Chem. Japan*, vol. 41, no. 3, pp. 173-180 (2007) (in Japanese)
8. N. Ojima. Image Analysis of Skin Color Using Independent Component Analysis and Its Application to Melanin Pigmentation Analysis, *J. Soc. Cosmet. Chem. Japan*, Vol.41, No.3, pp. 59-166 (2007) (in Japanese)
9. S. OE, T. KASHIWAGI, Imaging of Frequency Information of Color Image and its Applications, *Journal of Institute of Image Electronics Engineers*, vol.36, no.4, pp.530-535 (2007) (in Japanese)
10. Scalar Corporation, USB Microscope M3, <http://www.scalar.co.jp/products/m3.php?cat=education>

The 16th International Conference on Biomedical
Engineering

ICBME 2016, 7th to 10th December 2016, Singapore

Goh, J.; Lim, C.T.; Leo, H.L. (Eds.)

2017, XVIII, 135 p. 108 illus., Softcover

ISBN: 978-981-10-4219-5